Video Article

Localization of the Locus Coeruleus in the Mouse Brain

Katharina Schmidt[1], Bilal Bari[2], Martina Ralle[3], Clorissa Washington-Hughes[1], Abigael Muchenditsi[1], Evan Maxey[4], Svetlana Lutsenko[1]

[1]Department of Physiology, Johns Hopkins University, School of Medicine

[2]Department of Neuroscience, Johns Hopkins University

[3]Department of Molecular and Medical Genetics, OHSU

[4]X-ray science division, Advanced Photon Source, Argonne National Laboratory

Correspondence to: Katharina Schmidt at kschmi25@alumni.jh.edu

URL: https://www.jove.com/video/58652
DOI: doi:10.3791/58652

Keywords: Neuroscience, Issue 145, Brain, locus coeruleus, metals, immunohistochemistry, X-ray fluorescence microscopy, norepinephrine, copper, DBH, TH, ATP7A, ATP7B

Date Published: 3/7/2019

Citation: Schmidt, K., Bari, B., Ralle, M., Washington-Hughes, C., Muchenditsi, A., Maxey, E., Lutsenko, S. Localization of the Locus Coeruleus in the Mouse Brain. *J. Vis. Exp.* (145), e58652, doi:10.3791/58652 (2019).

Abstract

The locus coeruleus (LC) is a major hub of norepinephrine producing neurons that modulate a number of physiological functions. Structural or functional abnormalities of LC impact several brain regions including cortex, hippocampus, and cerebellum and may contribute to depression, bipolar disorder, anxiety, as well as Parkinson disease and Alzheimer disease. These disorders are often associated with metal misbalance, but the role of metals in LC is only partially understood. Morphologic and functional studies of LC are needed to better understand the human pathologies and contribution of metals. Mice are a widely used experimental model, but the mouse LC is small (~0.3 mm diameter) and hard to identify for a non-expert. Here, we describe a step-by-step immunohistochemistry-based protocol to localize the LC in the mouse brain. Dopamine-β-hydroxylase (DBH), and alternatively, tyrosine hydroxylase (TH), both enzymes highly expressed in the LC, are used as immunohistochemical markers in brain slices. Sections adjacent to LC-containing sections can be used for further analysis, including histology for morphological studies, metabolic testing, as well as metal imaging by X-ray fluorescence microscopy (XFM).

Video Link

The video component of this article can be found at https://www.jove.com/video/58652/

Introduction

The locus coeruleus (LC) is an important region in the brainstem and a major site of norepinephrine (NE) production[1]. The LC sends projections throughout the brain[2] to the cortex, the hippocampus and the cerebellum[3] and regulates major physiological processes, including circadian rhythm[4,5], attention and memory[6], stress[7], cognitive processes[8], and emotion[9,10]. Dysfunction of LC has been implicated in neurological and neuropsychiatric disorders[11], including Parkinson disease[12,13,14], Alzheimer disease[14], depression[15,16,17], bipolar disorder[18,19], and anxiety[20,21,22,23,24]. Given these roles, analysis of LC is crucial to studying its function and dysfunction.

Mice are widely used for studies of physiologic and pathophysiologic processes. Due to their small size, the mouse LC has an average diameter of ~300 µm, leading to difficulty locating the structure. During brain sectioning, the LC can easily be missed in either coronal or sagittal sections. Available studies describing identification of LC in animals do not offer a step-by-step protocol that a non-expert can follow[1,25]. Thus, to offer guidance for the localization of LC, we describe a protocol that we developed to locate this region in the mouse brain for several applications (**Figure 1, Figure 2, Figure 3**). The protocol applies carefully controlled brain sectioning and immunohistochemical detection of DBH[26,27], or alternatively TH[24], both enzymes highly enriched in the LC[28]. Once LC is located by immunohistochemistry, adjacent brain slices can be used for further studies, including morphological and metabolic analyses, as well as metal imaging studies via X-ray fluorescence microscopy (XFM)[29]. We describe XFM as an example in this protocol (**Figure 3**).

Protocol

Studies of animals was approved by Johns Hopkins University Animal Care and use (ACUC) protocol number M017M385.

1. Brain Slicing

1. To immobilize, anesthetize mice by the application of 3% isoflurane.
    1. Soak a cotton ball with drops of isoflurane and place it in a 15 mL microcentrifuge tube. Place the animal's nose into the tube and allow it to inhale the isoflurane. Check for the depth of anesthesia by the lack of response to toe-pinch.
2. Place the animal on its back and immobilize it by pinning its extremities down with a T pin while having access to its abdomen.

3. Cut the animal with surgical scissors by making a snip from the abdominal skin and cut through the skin in the thorax region. Pin the skin down using T pins. Then break the peritoneal membrane up to the thorax. Expose the heart by cracking the thoracic cavity and cutting the diaphragm.
4. Cut the right atrium to allow the blood to flow out of the animal. Insert a 10 mL syringe with a 25-gauge needle into the left ventricle and perfuse with 10 mL of phosphate-buffered saline (PBS).
   NOTE: This allows the solution to flow through systemic circulation and exit through the right atrium.
5. Remove the 10 mL syringe and insert a 25-gauge needle attached to the 60 mL syringe. Perfuse through the left ventricle with 50 mL of ice cold 4% paraformaldehyde (PFA).
   1. Prepare ice cold 4% PFA solution by diluting 10% PFA solution in H_2O and chilling the final 4% PFA solution at 4 °C.
6. Isolate the head of the mouse and remove the brain from the skull.
   1. Cut the skin from the neck, and then cut towards the eyes to expose the skull. Crack the skull from the neck to the nose, and then from one eyeball to the other. Peel the skull out and excise the whole brain.
7. Incubate the brain in 4% PFA for 24 h at 4 °C.
8. Transfer the brain with forceps into a 50 mL conical tube filled with 25 mL of 30% sucrose solution. Keep it at 4 °C for 48-72 h until the brain sinks to the bottom of tube.
9. Cut the brain with an adult mouse brain slicer matrix coronal through the midbrain (~3 mm posterior of bregma). Keep the brain section containing the brainstem.
   NOTE: This will result in two brain sections – one containing most of cortex (anterior of the cut) and one containing the brainstem/cerebellum (posterior of the cut). Use the brainstem section for the following steps.
10. Embed the brainstem section with the cut surface placed on the bottom of an embedding mold, surrounded by optimal cutting temperature compound (OCT); move the embedded brain to a -80 °C freezer and freeze for at least 12 h – until further use.
11. Cutting at the cryostat: place the embedding mold containing the brain in OCT into the cryostat; incubate it in the cryostat for several hours to adjust the temperature of the brain block to that of the cryostat.
12. Peel away the embedding mold to expose the OCT block containing the brain.
13. Use razor blades to remove excess of OCT from the surface of the block without touching the brain.
14. Mount the OCT block on the chuck of the cryostat, exposing the cut surface of the brain toward the front.
15. Adjust the cut surface of the brain so that it is oriented in parallel to the razorblades of the cryostat.
16. Trim the brain beginning at the medulla, cutting 100 µm sections rostrally.
17. Trim rostrally until the cerebellum and brainstem cut as one continuous slice. Begin collecting slices at 50 µm thickness.
    NOTE: As one trims rostrally from the medulla, the brainstem and cerebellum will cut as two separate sections. In rostral sections, the brainstem and cerebellum will eventually merge at the level of the 4th ventricle. Once the lateral edges of the 4th ventricle are well-formed, then the cerebellum and brainstem will come out as one continuous slice.
    1. Collect OCT-surrounded brain slice with forceps and place it in a well of a 24-well plate filled with PBS (**Figure 2a**). The LC will be most prominent when the cerebellum and inferior colliculus meet one another at ~-5.52 mm posterior of bregma (**Figure 1b**).
       NOTE: The most anterior part of LC will disappear once the cerebellum has been fully sectioned and no longer surrounds the inferior colliculus at ~-5.34 mm posterior of bregma (**Figure 1c**).

2. Immunohistochemistry for Dopamine β-Hydroxylase or Tyrosine Hydroxylase (Figure 2)

1. Day 1
   1. Wash the selected slices three times for 5 min in PBS.
   2. Permeabilize for 24 h in 0.5% phosphate buffered saline with detergent (PBSD) at 4 °C.
      1. Dilute 125 µL of detergent in 25 mL of PBS.
2. Day 2
   1. Wash slices three times for 5 min in 0.5% PBSD.
   2. Add the primary antibody, anti-DBH or anti-TH for 18 h at a dilution of 1:500 in 0.5% PBSD at 4 °C.
3. Day 3
   1. Wash slices three times for 10 min in 0.5% PBSD.
   2. Add the desired secondary antibody (488 donkey anti-rabbit for green fluorescence) at a dilution of 1:1000 in 0.5% PBSD for 16 h.
   3. Wrap the 24 well plate in aluminum and place at 4 °C.
   4. Wash slices three times for 5 min in 0.5% PBSD.
   5. Wash for 5 min in PBS.
   6. Transfer slices with a pencil brush into a water container.
   7. Mount slices floating in water on charged slides.
   8. Coverslip sections with hard-set mounting media (without DAPI).
   9. Dry the mounted brain sections for 30 min at room temperature.
   10. Image brain slices at a confocal or fluorescent microscope with settings to detect signal from appropriate secondary antibody fluorophore wavelength.
   11. Adjust the microscope to the focal plane of the brain slice and take a single image at 10X magnification.
   12. To locate a possible LC region in the brain slice, use the 4th ventricle for orientation; the cerebellum is located above the ventricle, pons and brainstem are found below[30].
   13. To locate the LC, focus on the lateral edges of the 4th ventricle; the LC originates from the edges of the 4th ventricle and points toward the pons/ brainstem region (**Figure 2b, 2c**).

14. Following imaging and localization of the LC in certain brain slices, store slides containing brain slices at 4 °C.

3. Detection of the LC in Brain Slices

1. To locate the brain section containing the LC, slice the mouse brain as described above and collect sections in PBS filled 24 well dishes, as shown in **Figure 2a**.
    1. Place one brain section per well to allow for the proper localization of the LC.
2. Collect a total of 48 brain slices that will be immunostained per brain.
   NOTE: All the wells of the two dishes shown in **Figure 2a** contain brain slices from one animal.
3. Immunostain every third to fifth slice for DBH, or TH. Preferably, perform immunohistochemistry of those brain slices that are adjacent to those that are assayed further (via X-ray fluorescence microscopy, XFM).
   NOTE: This procedure allows for exact localization of the LC in the final assay slices (**Figure 2a**; labeled with numbers between the wells).
4. Adjust the number of brain slices that are immunostained depending on the application, *e.g.*, whether they require exact location of the center and edge of the LC, or just a rough approximation.
5. Following immunohistochemistry, detect brain slices containing LC via a characteristic pattern of expression at both sides of the 4th ventricle (**Figure 2b, 2c**). Magnification of the DBH signal in the LC of consecutive brain slices is shown in **Figure 2d, 2e**; the magnified image of the LC that is stained for TH is shown in **Figure 2f.**
6. Use the sections adjacent to those containing LC for further studies - in this case for XFM to quantify metal levels (**Figure 3**).
7. To perform XFM, collect 10-30 µm (depending on the setup) thin coronal brain slices on thin polymeric film with which they can be mounted on sample holders and imaged at the synchrotron.
8. Store brain slices which are prepared on thin polymeric film for XFM at room temperature and perform XFM.

4. Metal Imaging in the LC via XFM

1. Slice example mouse brain as described above, determine LC, and measure metal levels via XFM from these brain slices containing the LC.
2. Image elemental distributions on beamline 2-ID-E at the Advanced Photon Source (Argonne National Laboratory, Argonne IL).
3. Record data 'on the fly' as described previously[31].
4. Determine elemental concentrations in brain slices containing the LC using the program MAPS[32,33].

Representative Results

Changes in metal homeostasis (such as Cu, Fe, Zn, and Mn) are often observed in neurologic disorders, including changes in the LC[34,35]. Thus, determining metal levels in the brain is necessary for understanding of disease mechanisms. The brain sections generated using the described protocol can be used to quantify the levels of Cu and other metals in the LC and compare them to the levels in regions outside of the LC. (**Figure 3**). In our example, the brain slice that was cut through the LC, phosphate, potassium, chloride and copper was measured. Only copper was specifically elevated in the LC. Higher resolution XFM imaging (not shown here) can also be performed for detection of subcellular distribution of metal levels. Further possible applications of this protocol include the detection of abundance and intracellular distribution of DBH (**Figure 2b, 2d, 2e**), TH (**Figure 2c, 2f**), and other proteins expressed in the LC individually or in the co-staining assays, studies of LC morphology and neuronal density.

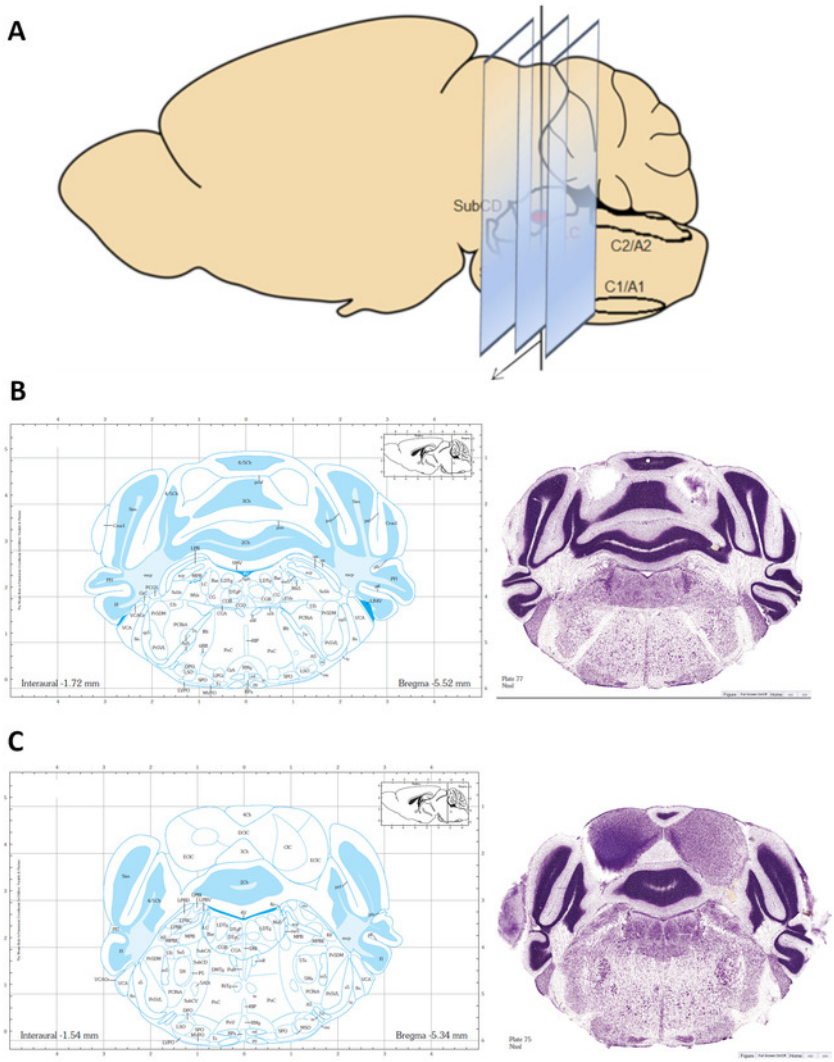

Figure 1: Localization of LC in the mouse brainstem. (**a**) Schematic demonstrating the region of the brainstem that will be sectioned to localize the LC. (**b**) Based on the Paxinos and Franklin brain atlas[30], LC will be most prominent when the cerebellum and inferior colliculus meet one another (-5.52 mm posterior of bregma). The left image shows a coronal section cut through the LC, while the right image demonstrates localization of LC on the lateral edges of the 4th ventricle via Nissl staining. (**c**) The most anterior part of LC will disappear once the cerebellum has been fully sectioned and no longer surrounds the inferior colliculus (-5.34 mm posterior of bregma). Nissl staining on the right image shows that LC is only marginally present in this coronal slice. Please click here to view a larger version of this figure.

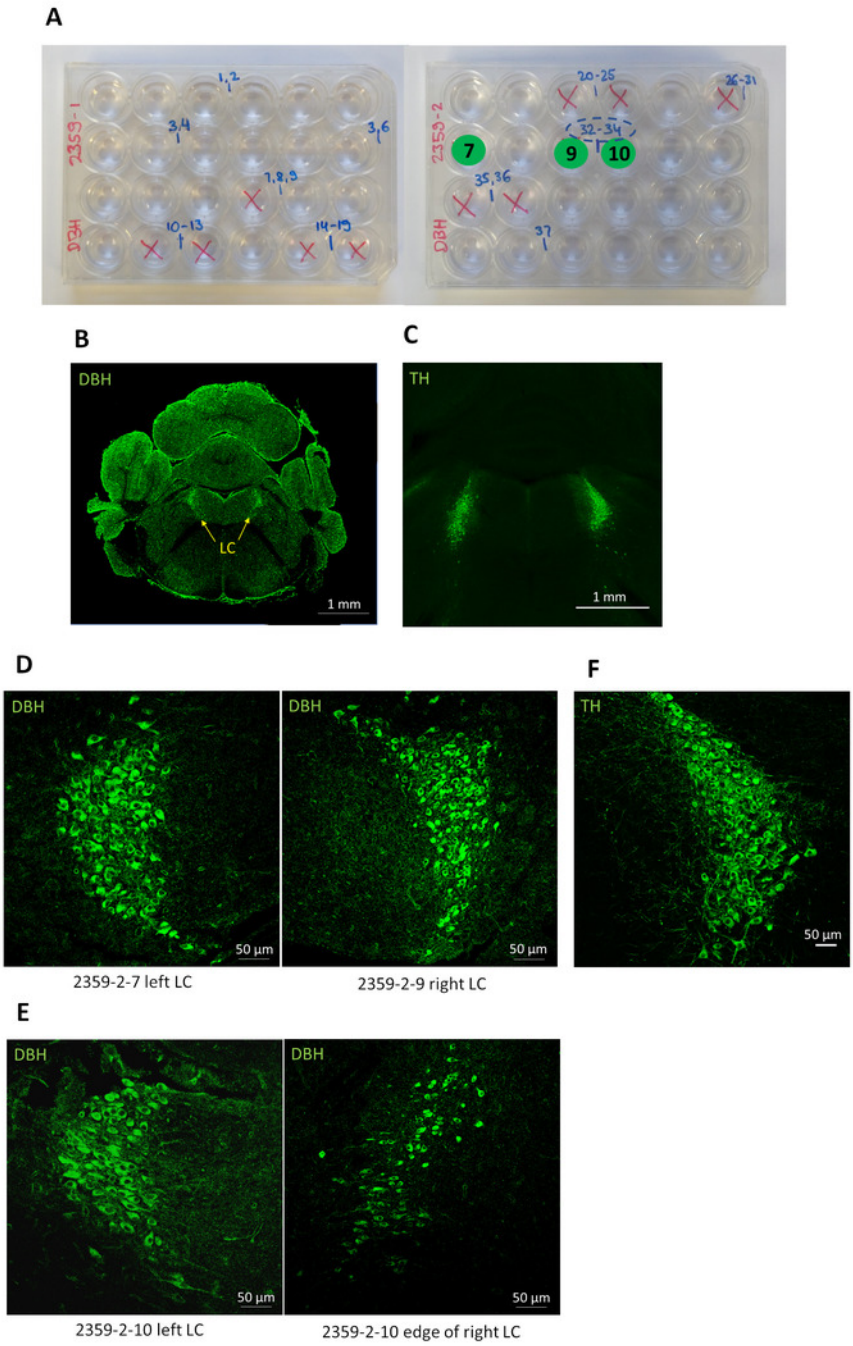

Figure 2: Detection of LC by immunostaining brain slices for DBH or TH. (**a**) One mouse brain was sectioned into 50 µm slices around the brain stem and collected in two 24 well dishes. Every 5th to 8th collected brain slice was mounted on film covered coverslip for imaging via XFM. These slices are labeled with blue numbers between the wells. Adjacent slices floating in PBS were immunostained for DBH to detect LC (labeled with red cross on wells). Green circles denote slices positive for DBH signal, and thus contain LC. (**b**) A coronal brain slice containing LC was immunostained with DBH and imaged on a confocal microscope. The image shows strong signal in the LC (in green). (**c**) A coronal slice containing LC was immunostained for tyrosine hydroxylase (TH) and imaged on a fluorescent microscope. Image shows strong signal for both left and right LC. (**d**) Slices were immunostained for DBH, and slices 7 (on the left) and 9 (on the right) contained LC. Adjacent sections were selected for XFM analysis. (**e**) Slice 10 also showed LC. In this section, the left LC was cut through its center while the right LC was captured at its anterior-most edge. (**f**) A section containing LC was immunostained for TH and imaged on a confocal microscope. Image shows TH expressing neurons in the LC labeled in green. Please click here to view a larger version of this figure.

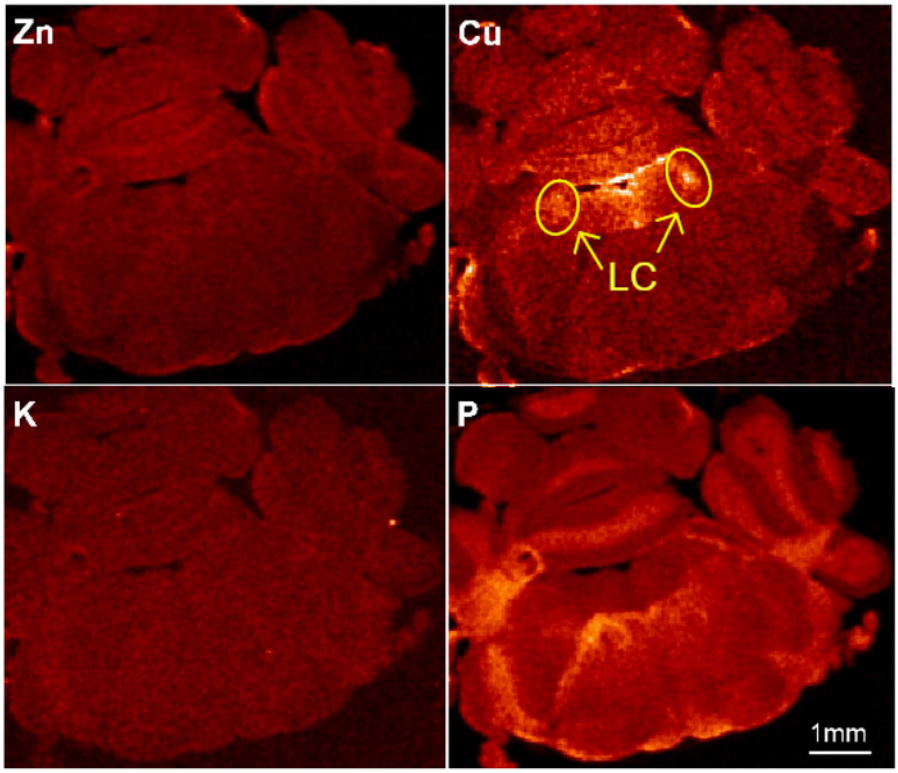

Figure 3: Imaging of metal levels in the LC. The brain of a male 12-week-old mouse with a knockout of Cu-transporter ATP7B was isolated and prepared as described in this protocol. Non-stained slices adjacent to LC-containing sections were taken and metal levels were measured via XFM. Cu levels were specifically increased in the LC (labeled with yellow arrows) as compared to the surrounding brain region, while other elements (K, P, and Cl) were unchanged. Please click here to view a larger version of this figure.

Discussion

Properly orienting the specimen is a crucial step in this protocol. Because we are using anatomical features of the dorsal surface of the brain to locate LC (boundary between cerebellum and inferior colliculus), it is important that the sections be aligned properly. This requires care in properly setting the brain into the mouse brain slicer matrix. We recommend cutting ~500 µm more tissue anterior and posterior to LC to avoid missing the nucleus. The most common mistake is to cut too few sections that results in missing the LC entirely. Thus, for one's first time following this protocol, we recommend cutting more sections than necessary. Careful study of the brain atlas images prior to staining is very helpful. The appearance of the brainstem changes appreciably every few hundred microns and, with some experience, it is possible to know what sections are worth staining simply by the macroscopic appearance.

During the process of localizing the LC, there might be variations in the signal depending on how well the brain was oriented during sectioning. When cutting through the center of the LC, the signal is bright and covers a larger area as compared to the edge of the LC, which will show up as a signal over a much smaller area. In the case that coronal slices are slightly tilted, the LC of one side of the 4th ventricle might be apparent and the one on the other side might only be visible in an adjacent slide. Thus, one cannot always expect the appearance of both LC regions at maximum intensity within one brain slice. This artifact can be avoided by cutting the brain exactly coronal in the mouse brain slicer matrix and carefully embedding the brain into the cubical embedding mold with OCT.

Immunostaining, at least with the anti-tyrosine hydroxylase antibody, is extremely forgiving and, in our experience, works on sections up to 100 µm in thickness. We have found that blocking solution is not necessary for high signal-to-noise staining of LC, reducing cost and reducing the amount of time needed to locate LC. In our experience, the staining protocol can be sped up – albeit with reduced quality and penetrance of staining – by reducing permeabilization to 2 h, primary antibody for 8 h, and secondary antibody for 2 h. Additionally, if one is simply interested in locating LC (*e.g.*, for validating injection of a virus/tracer), sections from a fixed brain can be cut on a vibratome at 100 µm thickness.

One limitation of this protocol is it, by design, requires euthanizing the animal and removing the brain. Therefore, it is not useful for in vivo localization (*e.g.*, electrophysiologic recordings). Another limitation is that this protocol requires PFA fixation which might alter the native state of the tissue. These alterations include the elemental content such as copper, calcium, iron and zinc[36]. The actual alteration of metal distribution caused by PFA fixation may be tested in one sample which can be run in parallel to a non-fixed sample. A comparison of the metal distribution between these two samples will provide evidence on the effect of PFA fixation on the distribution of the metal which is of interest in a certain study. If PFA fixation must be avoided, the general principle of this protocol (locating LC by immunostaining and using adjacent sections for follow-up experiments) can be extended to frozen sections without fixation.

We note that this protocol is largely a refinement of existing methods to solve this problem. The novelty exists in tailoring previous approaches to locate a very small, easily missed nucleus. We expect that this protocol can be easily modified and extended based on need (*e.g.*, using transgenic animals expressing fluorophores in LC to avoid immunostaining).

Disclosures

None.

Acknowledgments

We thank Abigael Muchenditsi for the maintenance of the mouse colony. Use of the Advanced Photon Source at Argonne National Laboratory was supported by the U.S. Department of Energy, Office of Science, Office of Basic Energy Sciences, under contract number: DE-AC02-06CH11357. We thank Olga Antipova and Dr. Stefan Vogt for user support and assistance at the Advanced Photon Source. This work was funded by the National Institute of Health grant 2R01GM101502 to SL.

References

1. Robertson, S. D., Plummer, N. W., de Marchena, J., & Jensen, P. Developmental origins of central norepinephrine neuron diversity. *Nature neuroscience.* **16**, 1016-1023 (2013).
2. Kobayashi, R. M., Palkovits, M., Jacobowitz, D. M., & Kopin, I. J. Biochemical mapping of the noradrenergic projection from the locus coeruleus. A model for studies of brain neuronal pathways. *Neurology.* **25**, 223-233 (1975).
3. Olson, L., & Fuxe, K. On the projections from the locus coeruleus noradrealine neurons: the cerebellar innervation. *Brain research.* **28**, 165-171 (1971).
4. Costa, A., Castro-Zaballa, S., Lagos, P., Chase, M. H., & Torterolo, P. Distribution of MCH-containing fibers in the feline brainstem: Relevance for REM sleep regulation. *Peptides.* **104**, 50-61 (2018).
5. Semba, J., Toru, M., & Mataga, N. Twenty-four hour rhythms of norepinephrine and serotonin in nucleus suprachiasmaticus, raphe nuclei, and locus coeruleus in the rat. *Sleep.* **7**, 211-218 (1984).
6. Takeuchi, T. *et al.* Locus coeruleus and dopaminergic consolidation of everyday memory. *Nature.* **537**, 357-362 (2016).
7. Korf, J., Aghajanian, G. K., & Roth, R. H. Increased turnover of norepinephrine in the rat cerebral cortex during stress: role of the locus coeruleus. *Neuropharmacology.* **12**, 933-938 (1973).
8. Sara, S. J., & Segal, M. Plasticity of sensory responses of locus coeruleus neurons in the behaving rat: implications for cognition. *Progress in brain research.* **88**, 571-585 (1991).
9. Markevich, V. A., & Voronin, L. L. [Synaptic reactions of sensomotor cortex neurons to stimulation of emotionally significant brain structures]. *Zhurnal vysshei nervnoi deiatelnosti imeni I P Pavlova.* **29**, 1248-1257 (1979).
10. File, S. E., Deakin, J. F., Longden, A., & Crow, T. J. An investigation of the role of the locus coeruleus in anxiety and agonistic behaviour. *Brain research.* **169**, 411-420 (1979).
11. Pamphlett, R. Uptake of environmental toxicants by the locus ceruleus: a potential trigger for neurodegenerative, demyelinating and psychiatric disorders. *Medical hypotheses.* **82**, 97-104 (2014).
12. Wang, J. *et al.* Neuromelanin-sensitive magnetic resonance imaging features of the substantia nigra and locus coeruleus in de novo Parkinson's disease and its phenotypes. *European journal of neurology.* **25**, 949-e973 (2018).
13. Oliveira, L. M., Tuppy, M., Moreira, T. S., & Takakura, A. C. Role of the locus coeruleus catecholaminergic neurons in the chemosensory control of breathing in a Parkinson's disease model. *Experimental neurology.* **293**, 172-180 (2017).
14. Zarow, C., Lyness, S. A., Mortimer, J. A., & Chui, H. C. Neuronal loss is greater in the locus coeruleus than nucleus basalis and substantia nigra in Alzheimer and Parkinson diseases. *Archives of neurology.* **60**, 337-341 (2003).
15. Chandley, M. J. *et al.* Gene expression deficits in pontine locus coeruleus astrocytes in men with major depressive disorder. *Journal of psychiatry & neuroscience : JPN.* **38**, 276-284 (2013).
16. Bernard, R. *et al.* Altered expression of glutamate signaling, growth factor, and glia genes in the locus coeruleus of patients with major depression. *Molecular psychiatry.* **16**, 634-646 (2011).
17. Gos, T. *et al.* Tyrosine hydroxylase immunoreactivity in the locus coeruleus is elevated in violent suicidal depressive patients. *European archives of psychiatry and clinical neuroscience.* **258**, 513-520 (2008).
18. Bielau, H. *et al.* Immunohistochemical evidence for impaired nitric oxide signaling of the locus coeruleus in bipolar disorder. *Brain research.* **1459**, 91-99 (2012).
19. Wiste, A. K., Arango, V., Ellis, S. P., Mann, J. J., & Underwood, M. D. Norepinephrine and serotonin imbalance in the locus coeruleus in bipolar disorder. *Bipolar disorders.* **10**, 349-359 (2008).
20. Borodovitsyna, O., Flamini, M. D., & Chandler, D. J. Acute Stress Persistently Alters Locus Coeruleus Function and Anxiety-like Behavior in Adolescent Rats. *Neuroscience.* **373**, 7-19 (2018).
21. Hirschberg, S., Li, Y., Randall, A., Kremer, E. J., & Pickering, A. E. Functional dichotomy in spinal- vs prefrontal-projecting locus coeruleus modules splits descending noradrenergic analgesia from ascending aversion and anxiety in rats. *eLife.* **6** (2017).
22. McCall, J. G. *et al.* CRH Engagement of the Locus Coeruleus Noradrenergic System Mediates Stress-Induced Anxiety. *Neuron.* **87**, 605-620 (2015).
23. Borges, G. P., Mico, J. A., Neto, F. L., & Berrocoso, E. Corticotropin-Releasing Factor Mediates Pain-Induced Anxiety through the ERK1/2 Signaling Cascade in Locus Coeruleus Neurons. *The international journal of neuropsychopharmacology.* **18** (2015).
24. Simone, J. *et al.* Ethinyl estradiol and levonorgestrel alter cognition and anxiety in rats concurrent with a decrease in tyrosine hydroxylase expression in the locus coeruleus and brain-derived neurotrophic factor expression in the hippocampus. *Psychoneuroendocrinology.* **62**, 265-278 (2015).
25. Carter, M. E. *et al.* Tuning arousal with optogenetic modulation of locus coeruleus neurons. *Nature neuroscience.* **13**, 1526-1533 (2010).

26. Fan, Y. *et al.* Corticosterone administration up-regulated expression of norepinephrine transporter and dopamine beta-hydroxylase in rat locus coeruleus and its terminal regions. *Journal of neurochemistry.* **128**, 445-458 (2014).
27. Xiao, T. *et al.* Copper regulates rest-activity cycles through the locus coeruleus-norepinephrine system. *Nature chemical biology.* **14**, 655-663 (2018).
28. Amaral, D. G., & Sinnamon, H. M. The locus coeruleus: neurobiology of a central noradrenergic nucleus. *Progress in neurobiology.* **9**, 147-196 (1977).
29. Ralle, M. *et al.* Wilson Disease at a Single Cell Level: intracellular copper trafficking activates compartment-specific responses in hepatocytes. *The Journal of Biological Chemistry.* **285**, 30875-30883 (2010).
30. Paxinos, G. *The Mouse Brain in Stereotaxic Coordinates.* Franklin, K. B. J. Boston, Amsterdam. (2013).
31. Bonnemaison, M. L. *et al.* Copper, zinc and calcium: imaging and quantification in anterior pituitary secretory granules. *Metallomics : integrated biometal science.* **8**, 1012-1022 (2016).
32. Nietzold, T. *et al.* Quantifying X-Ray Fluorescence Data Using MAPS. *Journal of visualized experiments : JoVE.* (2018).
33. Vogt, S. MAPS : A set of software tools for analysis and visualization of 3D X-ray fluorescence data sets. *J. Phys. IV France.* **104**, 635-638 (2003).
34. Davies, K. M. *et al.* Copper pathology in vulnerable brain regions in Parkinson's disease. *Neurobiology of aging.* **35**, 858-866 (2014).
35. Davies, K. M., Mercer, J. F., Chen, N., & Double, K. L. Copper dyshomoeostasis in Parkinson's disease: implications for pathogenesis and indications for novel therapeutics. *Clinical science (London, England : 1979).* **130**, 565-574 (2016).
36. James, S. A. *et al.* Quantitative comparison of preparation methodologies for X-ray fluorescence microscopy of brain tissue. *Analytical and bioanalytical chemistry.* **401**, 853-864 (2011).

